Original Article

JCBFM

Journal of Cerebral Blood Flow & Metabolism
2018, Vol. 38(10) 1741–1753

DOI: 10.1177/0271678X17714656
journals.sagepub.com/home/jcbfm

Lack of functional normalisation of tumour vessels following anti-angiogenic therapy in glioblastoma

Nina Obad[1,2,3], Heidi Espedal[1,3], Radovan Jirik[4], Per Oystein Sakariassen[1], Cecilie Brekke Rygh[1,5], Morten Lund-Johansen[2,6], Torfinn Taxt[1], Simone P Niclou[3,7], Rolf Bjerkvig[1,3,7] and Olivier Keunen[7]

Abstract

Neo-angiogenesis represents an important factor for the delivery of oxygen and nutrients to a growing tumour, and is considered to be one of the main pathodiagnostic features of glioblastomas (GBM). Anti-angiogenic therapy by vascular endothelial growth factor (VEGF) blocking agents has been shown to lead to morphological vascular normalisation resulting in a reduction of contrast enhancement as seen by magnetic resonance imaging (MRI). Yet the functional consequences of this normalisation and its potential for improved delivery of cytotoxic agents to the tumour are not known. The presented study aimed at determining the early physiologic changes following bevacizumab treatment. A time series of perfusion MRI and hypoxia positron emission tomography (PET) scans were acquired during the first week of treatment, in two human GBM xenograft models treated with either high or low doses of bevacizumab. We show that vascular morphology was normalised over the time period investigated, but vascular function was not improved, resulting in poor tumoural blood flow and increased hypoxia.

Keywords

Angiogenesis, bevacizumab, glioblastoma, hypoxia, perfusion, VEGF

Received 13 November 2016; Revised 11 April 2017; Accepted 18 April 2017

Introduction

Glioblastomas (GBMs) are highly heterogeneous tumours, characterised by angiogenesis and necrosis.[1] In 2009, the FDA approved bevacizumab, a monoclonal antibody against circulating vascular endothelial growth factor (VEGF), for second line treatment of patients with recurrent GBM. The accelerated approval was granted on the basis of two single arm trials, showing strong radiological responses in comparison to historical data,[2,3] assessed by the Macdonald criteria.[4] However, although progression-free survival (PFS) was prolonged, bevacizumab treatment did not improve overall survival (OS), when given alone or in combination with traditional chemotherapeutic regimens, whether for recurrent or newly diagnosed GBM.[5–7] The radiological response was attributed to a reduced blood brain barrier (BBB) permeability, rather than a true anti-tumour effect.[8] Several clinical trials in recurrent GBM have also attempted to combine bevacizumab therapy with alternative chemotherapeutic regimens.[9,10] The phase II BELOB trial,

[1]Department of Biomedecine, University of Bergen, Bergen, Norway
[2]Department of Neurosurgery, Haukeland University Hospital, Bergen, Norway
[3]KG Jebsen Brain Tumor research Center, University of Bergen, Bergen, Norway
[4]Institute of Scientific Instruments of the Czech Academy of Sciences, Brno, Czech Republic
[5]Bergen University College, Bergen, Norway
[6]Department of Clinical Science, University of Bergen, Bergen, Norway
[7]Norlux Neuro-Oncology Laboratory, Department of Oncology, Luxembourg Institute of Health, Luxembourg, Luxembourg

Corresponding author:
Olivier Keunen, Norlux Neuro-Oncology Laboratory, Department of Oncology, Luxembourg Institute of Health, 84,Val Fleuri, L-1526 Luxembourg, Luxembourg.
Email: olivier.keunen@lih.lu

for example showed improved OS in patients treated with a combination of lomustine and bevacizumab.[10] Unfortunately, a subsequent randomised phase III trial did not validate these results, leaving the future of anti-angiogenic treatment in GBM highly uncertain.[11]

According to Folkman's hypothesis, anti-angiogenic therapy should prevent the formation of new blood vessels, leading to a nutrient- and oxygen-deprived tumour that subsequently ceases to progress.[12] As tumour vessels are highly irregular, tortuous and leaky, the delivery of oxygen and nutrients is inefficient. Jain et al. proposed that anti-angiogenic therapy may lead to a transient window of tumour vessel normalisation, shortly after treatment initiation, with increased pericyte coverage and a thickening of the basal membrane, resulting in increased blood flow with improved oxygen and drug delivery.[13,14] In GBMs, preclinical studies have suggested that VEGF receptor 2 blockade can normalise the tumour vessels transiently by up-regulating angiopoietin 1 (Ang-1), leading to the stimulation and recruitment of pericytes with an increased tumour perfusion and decreased hypoxia.[15] It has also been proposed that this normalisation leads to a decreased interstitial pressure that facilitates drug delivery and an improved tumour oxygenation that increases tumour sensitivity to radiation.[16,17] In contrast, other studies indicate that anti-angiogenic treatment may lead to a reduced drug delivery caused by a restoration of the BBB.[18,19] Support for the former view is found among a subset of patients treated with cediranib, a VEGFR tyrosine kinase inhibitor (TKI), where increased tumour perfusion was observed in some patients.[20–22]

The proposed window of vascular normalisation is expected to occur transiently during the first days of treatment. In previous studies, our group has shown that bevacizumab treatment leads to morphological vessel normalisation without an increase in blood flow in human GBM patient-derived xenograft (PDX) models.[23,24] Since blood flow was evaluated several weeks after the initiation of the treatment, the transient window of vascular normalisation might have been missed in these studies. We thus designed the present study to establish whether our clinically relevant PDX models display such a window of vascular normalisation or not, by repeatedly assessing perfusion parameters during the early courses of bevacizumab treatment. We used two different models displaying the properties of a purely angiogenic and a mixed angiogenic/infiltrative phenotype, closely mimicking the features of clinical GBM. The animals were treated with bevacizumab in doses equivalent to their clinical counterparts or in lower doses to see whether tumour vessel normalisation represents a dose-dependent effect. Dynamic Contrast Enhanced magnetic resonance imaging (DCE-MRI) and histological analysis were used to assess vessel morphology and function, and Fluorine-18 Fluoromisonidazole (^{18}F-FMISO) PET was used to assess tumoural hypoxia.

The results presented here do not support the hypothesis that bevacizumab treatment causes a transient window of normalisation of tumour vessels function during the early stages of treatment. Instead, tumoural blood flow remained heterogeneous and inefficient during the period analysed. Moreover, ^{18}F-FMISO PET imaging showed a progressive increase in hypoxia in bevacizumab treated tumours, consistent with the reduced blood flow observed by magnetic resonance imaging (MRI).

Materials and methods

Xenograft models

A total of 37 nude male or female adult rats (rnu-/rnu-Rowett) were used for the studies (29 in the perfusion study and 8 in the hypoxia study). Group sizes were calculated according to expected variance in tumours growth, on the basis of previous similar studies. Animals were grouped in cages, fed ad libitum with standard food pellets, and their welfare was monitored through daily routine checks with increased daily frequency as animals were approaching the end stage. We used GBM spheroids generated from two different patients, Patient 3 (P3) and Patient 13 (P13) as previously described.[25] Tumour tissue was harvested during surgery and subsequently serially transplanted orthotopically in the animals. The tumours were passaged for either 32 (P3) or 7 (P13) generations in vivo. Both these models have been characterised in detail and recapitulate patient GBMs features by showing vascular proliferation, diffuse tumour cell infiltration and pseudo-palisading necrosis.[26] They have the following genomic characteristics; P3: + [Chr 7, Chr19, 20q], - [1q42-q43, Chr9, Chr10, 20 p] – [PIK3R1, CDKN2A/B]; P13: + [Chr7, Chr19, Chr20], - [6q16.2-16.3, Chr10, 17q12], – CDKN2A/B.[27] P13 is a highly angiogenic model with pronounced necrosis and little invasion. It displays contrast enhancement on T1-weighted images after injection of a gadolinium-based contrast agent, and responds to bevacizumab by a strong reduction in contrast enhancement. In comparison, P3, which is angiogenic as well, is more invasive and displays a less aggressive progression. It responds to bevacizumab by reduced contrast enhancement too, and has also been shown to increase glycolytic activity and invasion.[23,24] Pimonidazole staining shows increased hypoxia after bevacizumab treatment in both models. The key histological features of the P3 and P13 animal models are summarised in online Supplementary Figure S1.

The collection of biopsy tissue was approved by the regional ethical committee at the Haukeland University Hospital, Bergen, Norway (REK 013.09).

Intracranial implantation

All animal experiments were performed within a facility that was recently certified by the Association for Assessment and Accreditation of Laboratory Animal Care (AAALAC) International. All experiments were done in accordance with the Norwegian Animal Act. The protocols were approved by the Animal Welfare Body of the University of Bergen, and are in compliance with the ARRIVE guidelines (www.nc3rs.org.uk/arrive-guidelines). P3 or P13 spheroids were implanted stereotactically into the brains of nude immunodeficient rats, as described previously.[28] A burr hole was made 3 mm lateral and 1 mm posterior to the bregma on the right side and the spheroids were injected 3.5 mm below the cortical surface. The animals were euthanized when neurological signs were evident, by CO_2 inhalation, and perfused intracardially with 0.9% NaCl. The brains were removed, the caudal half was fixed in formalin and further processed for histological and immunohistological examination.

Bevacizumab treatment

Treatment was initiated once the tumours reached an average size of about 50 mm^3 as measured by MRI (typically 3 weeks after implantation for P13 and 4 weeks for P3). Animals were then divided randomly into treatment groups or controls. Bevacizumab (Avastin, Genentech, San Francisco, CA, USA) was injected i.v twice a week, at 10 mg/kg (high dose) or 5 mg/kg (low dose). The control animals received i.v saline following the same schedule. Separate groups of P13 implanted animals were used for the perfusion MRI studies and the hypoxia PET studies. The generic design of the studies is summarised in online Supplementary Figure S2, together with the number of animals used in each study.

Immunohistochemistry

Immunohistochemistry was performed as described previously.[24] Paraffin-embedded formalin-fixed tissue sections were de-paraffinized and brought to a temperature of 99°C for 20 min using a 10 mM citrate buffer at pH 6.0 or incubated with proteinase K diluted in 0.05 M Tris-Cl, at pH 7.5 and a temperature of 37°C for 10 min. The following primary antibodies were used during sections incubation: anti-von Willebrand factor (vWf) (1:1000; A0082; DAKO; Oslo, Norway), pimonidazole (1:200; Hypoxyprobe 9.7.11; HPI Inc; Burlington, MA, USA) and anti-human nestin (1:1000; MAB5326; Millipore; Billerica, MA, USA). Incubation of primary antibodies lasted 90 min at RT. A biotinylated secondary antibody (Vector Laboratories, Trondheim, Norway) was used for detection, amplified with Vectastain ABC Reagent (Vector). Development of the sections was done with 3′3-diaminobenzidine (DAB, DAKO Cytomation), according to the manufacturer's instructions. Pictures were obtained using a Nikon light microscope (Nikon Eclipse E600) and Nikon imaging software (Nikon NIS Elements v 4.11).

MRI

MRI was used to screen the animals after implantation and randomly split them into treatment and control groups according to tumour volumes. Extensive MRI sessions, including perfusion series, were then conducted longitudinally throughout the treatment. Images were acquired on a 7 T horizontal PharmaScan (Bruker Biospin) using either a quadratic volume coil or a four-channel surface coil designed for rat brain imaging. Animals were placed prone in a cradle and kept asleep with gas anaesthesia. We used 1–2% isofluorane mixed with 50% air for the first series of experiments, then switched to 50% O_2 or 1–3% sevofluorane mixed with 100% O_2, following an institutional decision motivated by animals stability, accelerated recovery, and unchanged blood flow and oxygenation. To avoid introducing experimental bias, groups compared within a study were always anesthetised with the same gas at all time points throughout the study. Body temperature was kept constant at 37°C and breathing was monitored throughout the scan sessions. The following acquisition parameters were used: (1) T2-weighted (T2w): method RARE, spatial resolution (SR) 137 μm × 137 μm × 1000 μm, echo time (TE) 36 ms, repetition time (TR) 3500 ms, rare factor (RF) 8, averages (AVG) 3; (2) T1-weighted (T1w): method RARE, SR 137 μm × 137 μm × 1000 μm, TE 9 ms, TR 1000 ms, RF 4, AVG 4; (3) Diffusion Weighted Imaging (DWI): method DtiEpi, SR 125 μm × 125 μm × 1000 μm, 3 directions, 6 b-values per direction from 0 to 1664 s/mm2; (4) Dynamic Contrast Enhanced (DCE): method FLASH, SR 156 μm × 156 μm × 1000 μm, TE 2.1 ms, TR 8 ms, FA 17°, time resolution 0.7 s, total scan time 12′48″, Contrast Agent 0.1 mmol/kg of Omniscan (GE Healthcare) injected intravenously after 25″. The animals were scanned every other day for 8 days, and treatment was started after the first scan (Day 1).

Analysis of the MRI data was performed in Paravision 5.1 (Bruker Biospin) and with routines custom developed in Matlab 2015b (MathWorks,

MA, USA) and C. Specifically, the perfusion analysis was based on the pharmacokinetic modelling of the DCE-MRI data using the adiabatic approximation of the tissue homogeneity model and blind deconvolution arterial input functions (AIFs), as described previously,[23,29] to separate the contributions of perfusion and vessels permeability changes to tumour physiology. The blind deconvolution AIFs were scaled so that a value known from the literature (12.8 mL/100 mL for the interstitial space + plasma fraction) was achieved for the reference tissue (left and right temporalis muscles).[23] Datasets that displayed poor signal-to-noise ratio (SNR) as a result of sub-optimal experimental conditions such as incomplete injection of the contrast agent or excessive rat motion, were excluded from the quantification. Tumour volume (TV) was defined as the part of the tumour visible on MRI, and measured by delineating tumour on consecutive 2D T2-weighted sections, multiplied by section thickness. Growth rate (GR) was calculated using the TV measurement at the first and last time points as $GR = 100 \times \log(TV_f/TV_0) / (t_f - t_0)$, where TV_f and TV_0 are the tumour volumes at the last and first time points, respectively, and $t_f - t_0$ is the difference in days between the time points. Tumour volumes are expressed in mm^3 and GR in '% per day'.

PET/CT imaging and data analysis

In vivo tumour hypoxia was evaluated by PET using in-house produced ^{18}F-fluoromisonidazole (^{18}F-FMISO) (ABX GmBH, Radeberg, Germany). PET/CT images were acquired on a small-animal nanoScan PET scanner (Mediso Medical Imaging Systems, Budapest, Hungary). An activity of ~30 MBq (31.8 ± 4.1) of ^{18}F-FMISO was injected in the tail-vein and the rats were left awake for 120 min prior to a 30 min acquisition scan (coincidence 1:5, normal count mode) as previously described.[24] Animals were anesthetised with 3% sevofluorane mixed in air throughout the scans, and monitored for breathing and temperature. CT semicircular scans (50 kVp, 300 ms, 480 projections) were performed for anatomical reference and attenuation correction of PET images. PET reconstruction was performed by Nucline nanoscan (Mediso Medical Imaging Systems) from list-mode using the following parameters: reconstruction algorithm Tera-Tomo 3D, full detector model, 4 iterations/6 subsets, 1:3 coincidence mode and a voxel size of 0.4 mm.

The images were quantified using InterView Fusion v3.01 (Mediso Medical Imaging Systems). A 3 mm sphere-shape volume of interest was placed in both the tumour and the contralateral hemisphere to calculate tumour-to-brain ratios using standard uptake value (SUV) mean.

Statistics

Individual animals were used as observations when assessing tumour volumes and tumour voxels were used as observations when assessing perfusion parameters, to account for the heterogeneity within the tumours. Mean values for each time point are reported for the treated and control animals. A Student's *t*-test was used to assess the statistical significance of differences between groups, calculated in Matlab (MathWorks). p Values < 0.05 were considered statistically significant.

Results

Tumour progression

Twenty-nine animals were used in the perfusion MRI studies, split for both the P3 and P13 models into controls versus treatment groups, as detailed in online Supplementary Figure S2. MRI showed a continuous growth in both tumour models during the time period of 1–8 days, for both the controls and the bevacizumab treated tumours in P13 implanted animals (Figure 1(a) and (b)) and P3 implanted animals (Figure 1(e) and (f)). Tumour volume progression during that time window was exponential for all models and treatment groups (Figure 1(c) and (g)). Quantification of tumour volumes indicated a tendency toward lower growth rate in the bevacizumab treated group compared to the controls for the P13 model (12% ± 2% versus 16% ± 2% per day) (Figure 1(d)). Changes were however not statistically significant for the small cohorts used. For the P3 implanted animals, the tendency toward smaller growth rate in the treated animals was less pronounced (12% ± 3% vs. 14% ± 4% per day) (Figure 1(h)), suggesting a weaker response to bevacizumab at the onset of treatment, possibly due to the less angiogenic and more infiltrative nature of this model. The changes were nevertheless not statistically significant either in the cohorts used.

We also acquired DWI data at each time point and calculated apparent diffusion coefficients (ADC), which have previously been related to cellularity, to see if longitudinal changes in ADC could inform us on a possible increase of the infiltrative compartment of the tumours. ADC was however stable for both tumour models over the time period investigated and no statistically significant changes were observed (data not shown).

Morphological normalisation of tumour vessels

DCE-MRI was used to obtain quantitative values of perfusion and vessel permeability parameters over

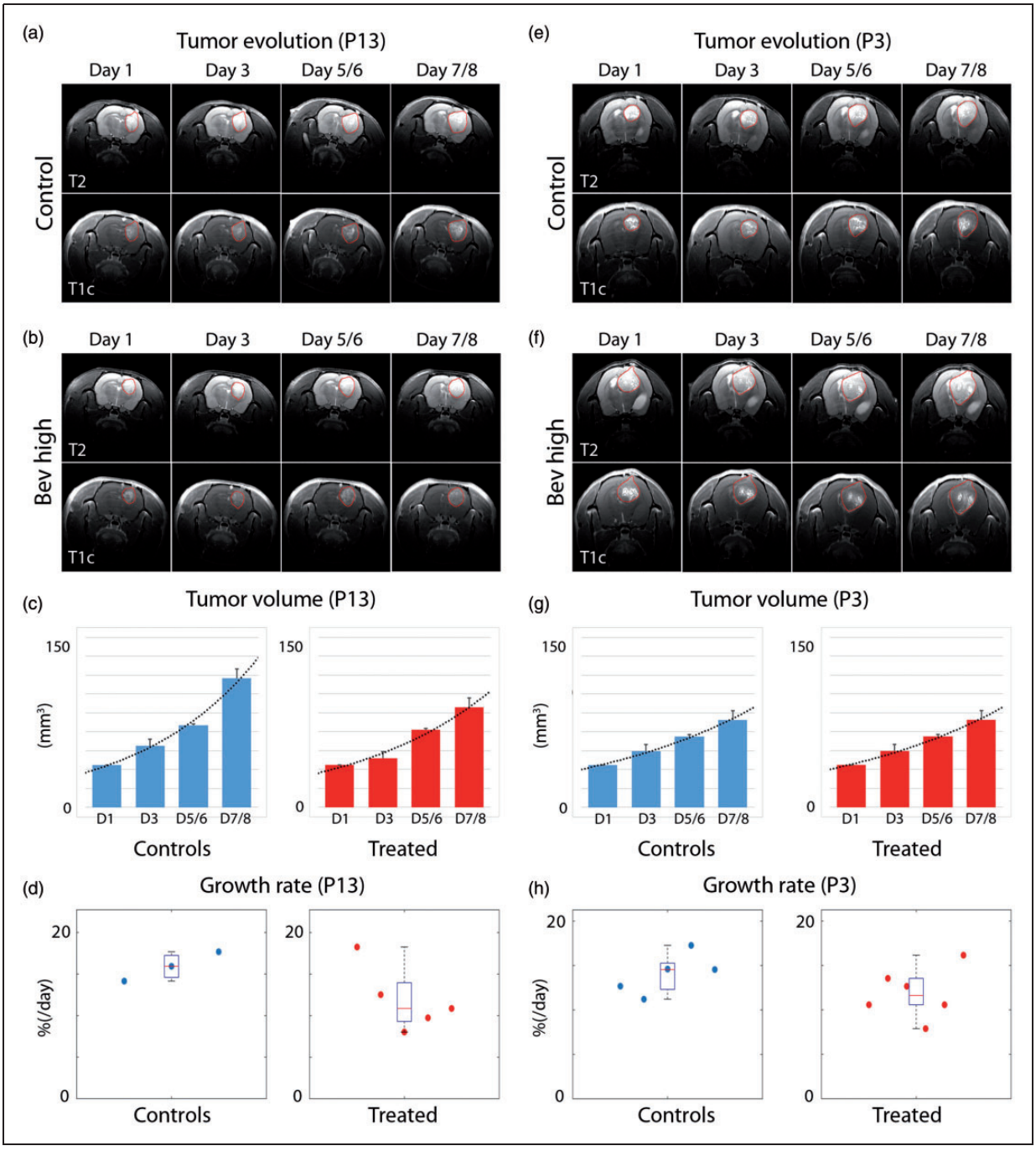

Figure 1. Tumor size evolution: Representative cases of tumour evolution for the animals implanted with the angiogenic P13 phenotype, showing one control (a), and one animal treated with high doses of bevacizumab (b). Images represent T2 weighted MRI acquisitions (top rows) and contrast enhanced T1 weighted MRI (bottom rows). Quantification of corresponding tumour volumes (c) and growth rates (d) for P13 animals per group. Whiskers boxes show percentile 25, median and percentile 75 values. Representative cases of tumour evolution for the animals implanted with the more infiltrative P3 phenotype, showing one control (e), and one animal treated with high doses of bevacizumab (f). Quantification of corresponding tumour volumes (g) and growth rates (h) for P3 animals per group. Tumour volumes show an exponential progression in all groups for P13 (c) and P3 (g) during the time window of observation. Growth rates were higher for controls than for bevacizumab treated animals in both the P13 (d) and the P3 (h) tumour models, and this difference was more pronounced for the more angiogenic P13 tumour model. Tumour volumes expressed in mm^3 and growth rates in % per day. Animals per group: P13 Controls-5, P13 Bev high-5, P3 Controls-5, P3 Bev high-6. High dose: 10 mg/kg. (Scale bars: ± SE).

time, and to assess if anti-angiogenic therapy induces a window of normalisation of tumour vessels for the two GBM models used. For the more angiogenic model (P13), high and low doses of bevacizumab were used to further evaluate whether this putative normalisation was associated with a dose-dependent effect. Mean tumour values as well as tumoural (voxels) values were examined to account for the spatial heterogeneity of the parameters within the tumour.

We observed that tumour blood volume (V_b) increased over time in the control (untreated) animals for the angiogenic P13 model, as illustrated by one representative animal in this group (Figure 2(a), top line). This increase was less pronounced in the treated animals, whether given high doses (10 mg/kg) or low doses (5 mg/kg) of bevacizumab (Figure 2(a), middle and bottom lines). Quantification of the mean tumoural V_b (Figure 2(b), top line) revealed a steady progression over time in the control animals, and for the treated animals a reduction first, followed by a steady progression. In comparison to controls, tumoural V_b mean values in the treated animals were 39% and 46% lower on Day 5/6 for the animals treated with 10 mg/kg doses of bevacizumab (Bev high) and those treated with the 5 mg/kg doses of bevacizumab (Bev low) groups, respectively ($p < 0.001$). Histogram analysis of tumoural V_b values distribution (Figure 2(b), bottom line) showed a progressive increase in the fraction of high V_b values (dark blue) compared to medium V_b (hatched blue) and low V_b (light blue) values over

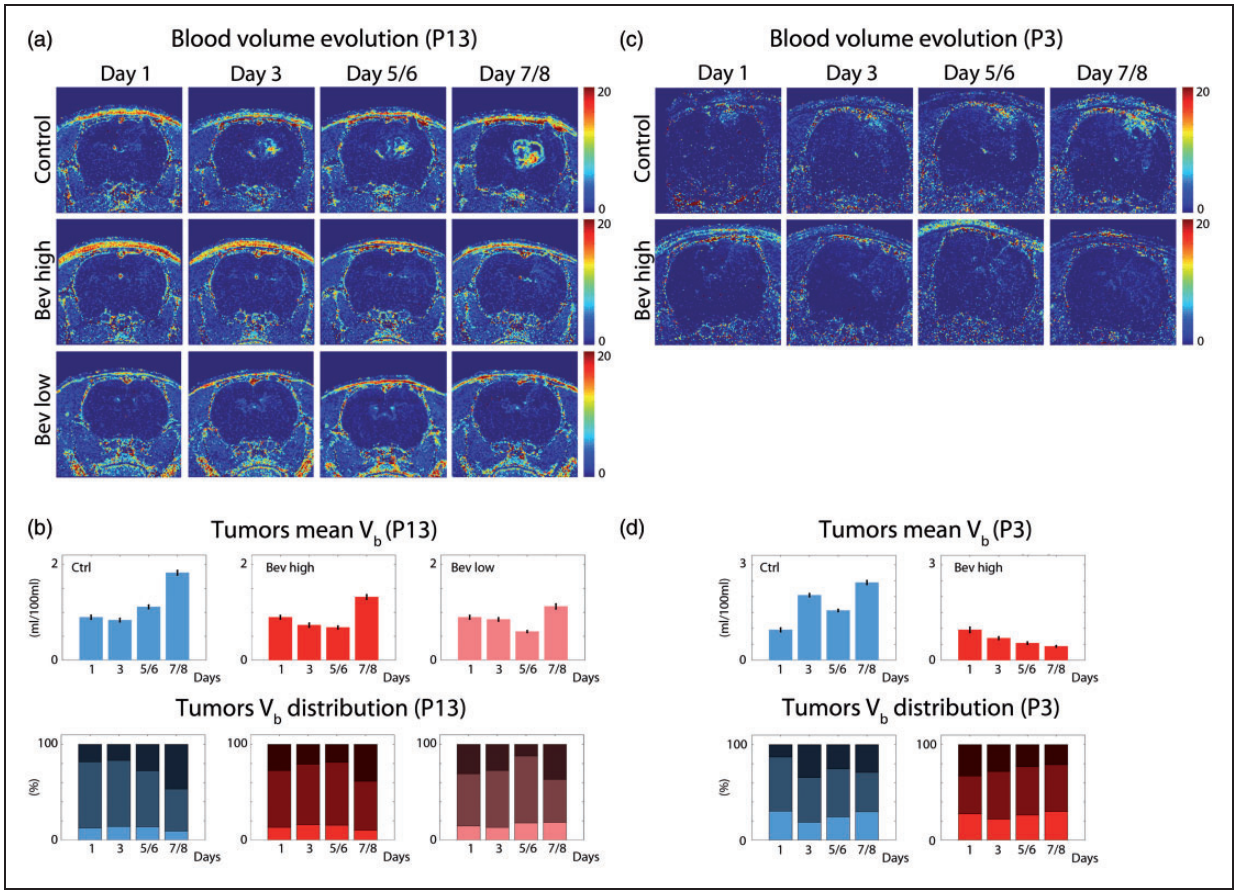

Figure 2. Tumoural blood volume evolution. (a) Illustrative maps of blood volume (V_b) evolution for animals implanted with the highly angiogenic P13 tumour model, showing one control (top line) and two animals treated with respectively high and low doses of bevacizumab (middle and bottom lines). (b) Quantification of tumour mean V_b for P13 animals (top line) and histogram analysis of tumoural V_b values distribution (bottom line). In comparison to controls, animals treated with bevacizumab high or low doses, show a reduced tumour mean V_b and a reduced fraction of high V_b values shortly after the start of the treatment, suggesting a normalisation of blood vessel morphology. Similar results are observed for the less angiogenic more infiltrative P3 model (c and d), where the normalisation window extends throughout the whole observation period. V_b expressed in absolute values of mL/100 mL of tissue. Thresholds for the high, medium and low values (dark, hatched and light blue/red) were defined by the 75% and 25% percentiles of the whole voxel population for the given tumour model. Animals per group: P13 Controls-5, P13 Bev high-5, P13 Bev low-5, P3 Controls-7, P3 Bev high-7. Bev high: 10 mg/kg, Bev low: 5 mg/kg.

time for the control animals. In the animals treated with high or low doses of bevacizumab, a reduction of the fraction of high V_b values was observed early after the start of the treatment, suggesting a possible morphological normalisation effect caused by the treatment.

For the less angiogenic and more infiltrative P3 model, tumour V_b also increased steadily over time for the control animals (Figure 2(c)), with mean tumour V_b and distribution showing more fluctuations (Figure 2(d)). For animals treated with high doses of bevacizumab, the normalisation effect suggested by progressive decrease of mean tumoural V_b and progressive reduction of the fraction of high V_b values, lasted throughout the whole observation period. In comparison to controls, mean tumoural V_b in the treated animals was 82% lower on Day 7/8 ($p < 0.001$).

The permeability of blood vessels was also assessed, using the permeability surface (PS) area product parameter that represents the product of the permeability (leakiness) of vessel wall by the area of vessel wall. Similarly to V_b, PS increased in the P13 control animals (Figure 3(a), top line). Quantification of mean tumoural PS (Figure 3(b), top line) revealed a sustained progression of this parameter over time in this group, with a progressive increased fraction of high PS values (Figure 3(b), bottom line). For the animals treated with bevacizumab, PS was more stable over time

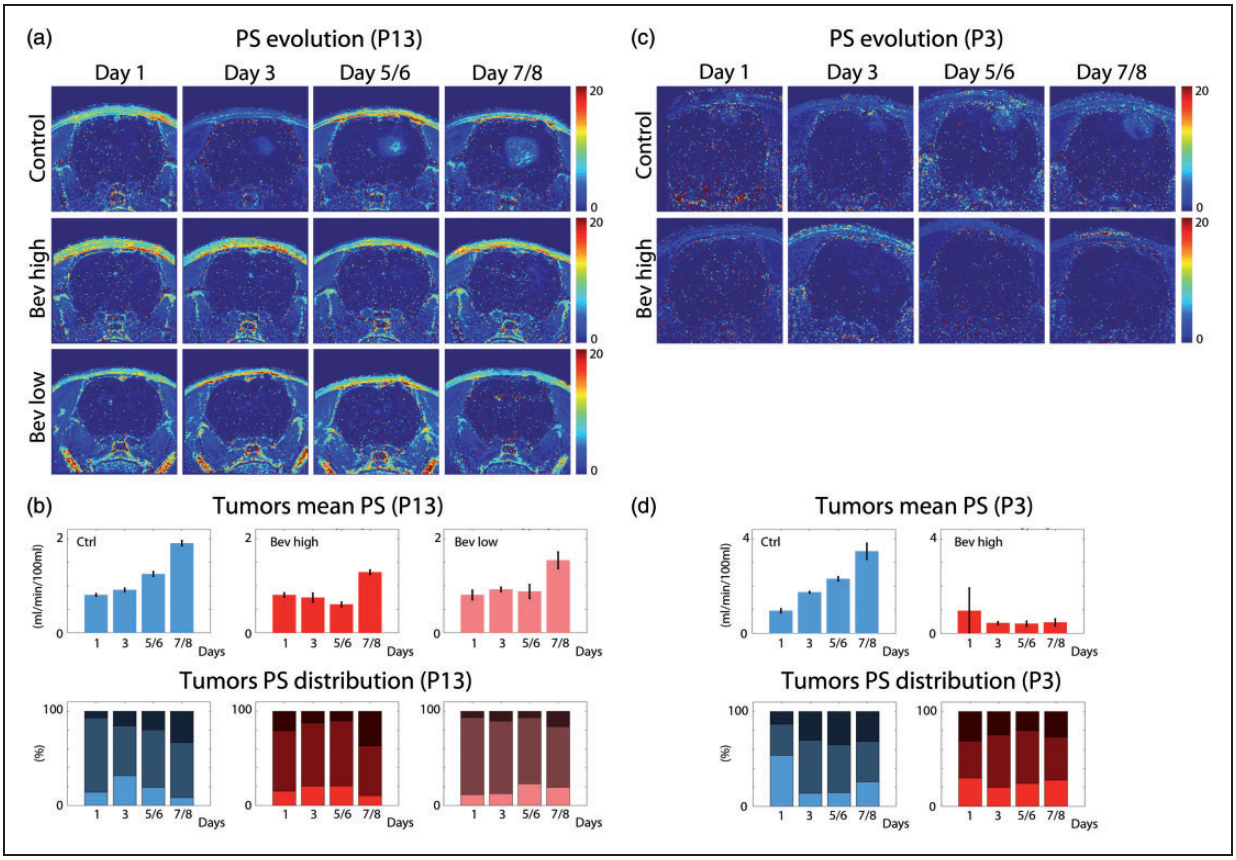

Figure 3. Tumoural vessel permeability evolution. (a) Illustrative maps of the permeability surface area product (PS) evolution for animals implanted with the highly angiogenic P13 tumour model, showing one control (top line) and two animals treated with respectively high and low doses of bevacizumab (middle and bottom lines). (b) Quantification of tumours mean PS for P13 animals (top line) and histogram analysis of tumoural voxels PS distribution (bottom line). In comparison to controls, animals treated with bevacizumab high or low doses, show a reduced tumour mean PS and a reduced fraction of high PS voxels shortly after the start of the treatment, again suggesting a normalisation of blood vessel morphology. For the less angiogenic, more infiltrative P3 model (c and d), the normalisation window extends throughout the whole observation period. Datasets displaying poor SNR as a result of experimental conditions, such as on Day 1 for the represented P3 Control (C), were not considered in the quantification. PS expressed in absolute values of mL/min/100 mL of tissue. Thresholds for the high, medium and low values (dark, hatched and light blue/red) were defined by the 75% and 25% percentiles of the whole voxels population for the given tumour model. Animals per group: P13 Controls-5, P13 Bev high-5, P13 Bev low-5, P3 Controls-7, P3 Bev high-7. Bev high: 10 mg/kg, Bev low: 5 mg/kg.

(Figure 3(a), middle and bottom lines). Quantification of mean tumoural PS for the animals treated with high doses of bevacizumab showed a reduction first, followed by a steady increase (Figure 3(b), top line), similar to what was observed for the tumoural blood volumes (Figure 2(b), top line). In comparison to controls, PS in this treatment group was 52% lower on Day 5/6 ($p < 0.001$). The distribution of tumoural PS (Figure 3(b), bottom line) showed a reduction of the high PS values fraction first, followed by a steady increase, again suggestive of a transient normalisation of this parameter following anti-angiogenic therapy. This effect was less pronounced for the animals treated with the low dose of bevacizumab.

For the less angiogenic, more infiltrative P3 model (Figure 3(c)), mean tumour PS also increased steadily in the controls and was more stable for the animals treated with high doses of bevacizumab (Figure 3(d), top line). In comparison to controls, PS in the treatment group was 82% lower on Day 7/8 ($p < 0.001$). The distribution of tumoural PS values showed a progressive increase of the fraction of high PS values in the controls, and a more stable or slightly decreasing fraction of high PS values in the bevacizumab treated animals (Figure 3(d), bottom line).

In many studies on brain tumour perfusion, K^{trans}, a parameter that represents the outflow of contrast agent from the vascular compartment to the tissue is used, to provide an indication of vessel permeability. It should however be noted that K^{trans} is also influenced by blood flow. This makes interpretation of changes in this parameter more complex, especially in studies involving treatments with anti-angiogenic agents that are known to interfere with vessel permeability. PS, on the contrary, is independent of blood flow, such that changes in PS more accurately reflect changes in the permeability of blood vessels. Nevertheless, the longitudinal changes in K^{trans} in our study closely followed those of PS (online Supplementary Figure S3). Thus, changes in vessel permeability, when further used in the text, can here indifferently be regarded as referring to changes in PS or K^{trans}.

Details of mean tumour V_b, PS and K^{trans} for all time points are provided in online Supplementary Tables S1 and S2, together with the ratio of values for bevacizumab treated versus control animals and associated *p*-values.

In summary, the longitudinal study on changes in blood volume and vessel permeability parameters suggests a morphological normalisation of the blood vessels early after the start of the anti-angiogenic therapy, whether given in high or low doses, for both the more angiogenic and the less angiogenic, more infiltrative, tumour phenotypes used in this study.

Functional normalisation of tumour vessels

For the P13 model, blood flow (F) fluctuated over time in the tumours of the control animals (Figure 4(a), top line), with a tendency of mean tumour F to slightly increase over time (Figure 4(b), top line), and a progressive increase of the high F voxels fraction (Figure 4(b), bottom line). In the treated animal groups, tumour F values fluctuated but to a lesser extent compared to controls (Figure 4(a), middle and bottom lines). In comparison to controls, animals treated with high doses of bevacizumab showed a more stable but lower increase in mean tumour F values (fluctuating from +47% to −6% during the observation window) and the fraction of high F values increased slightly (Figure 4(b)). For the animals treated with low doses of bevacizumab, the mean tumour F values kept fluctuating over time and also increased less than for the controls. Mean tumour F ranged from +47% to −39% in comparison to controls (with varying *p*-values at each time point) during the observation window. The distribution of F values also fluctuated over time with no clear evolutionary trend (Figure 4(b)).

For the P3 control animals (Figure 4(c), top line), both the mean tumour F and the fraction of high tumour F increased over time (Figure 4(d)). For the animals treated with high doses of bevacizumab (Figure 4(c), bottom line), mean tumour F values remained stable over time and was significantly lower than controls (down to 45% of controls on Day 7/8, $p < 0.001$). The fraction of high F values remained constant during the observation window (Figure 4(d)).

Details of mean tumour F for all time points are provided in online Supplementary Tables S1 and S2, together with the ratio of values for bevacizumab treated versus control animals and associated *p*-values.

We also quantified perfusion parameters in other regions to verify the consistency of the results obtained. Assessment of perfusion parameters in the contralateral brain is challenging because an uncompromised BBB results in limited leakage of the contrast agent and poor SNR with the method used. Quantification results in this region are therefore to be considered with caution. We thus additionally quantified perfusion parameters in the temporalis muscle where the SNR is much higher. Overall F, Vb and PS remained stable and homogeneous over time in the muscle. In comparison to tumours, F and Vb had a similar range of values while PS was higher in the muscles than in the tumours, for both models. All perfusion parameters seemed unaffected by the treatment in the muscles while they were reduced in the treated tumours. In the contralateral brain, F, Vb and PS also remained rather stable and homogeneous over time and were not affected by the treatment. Most parameters were significantly lower in

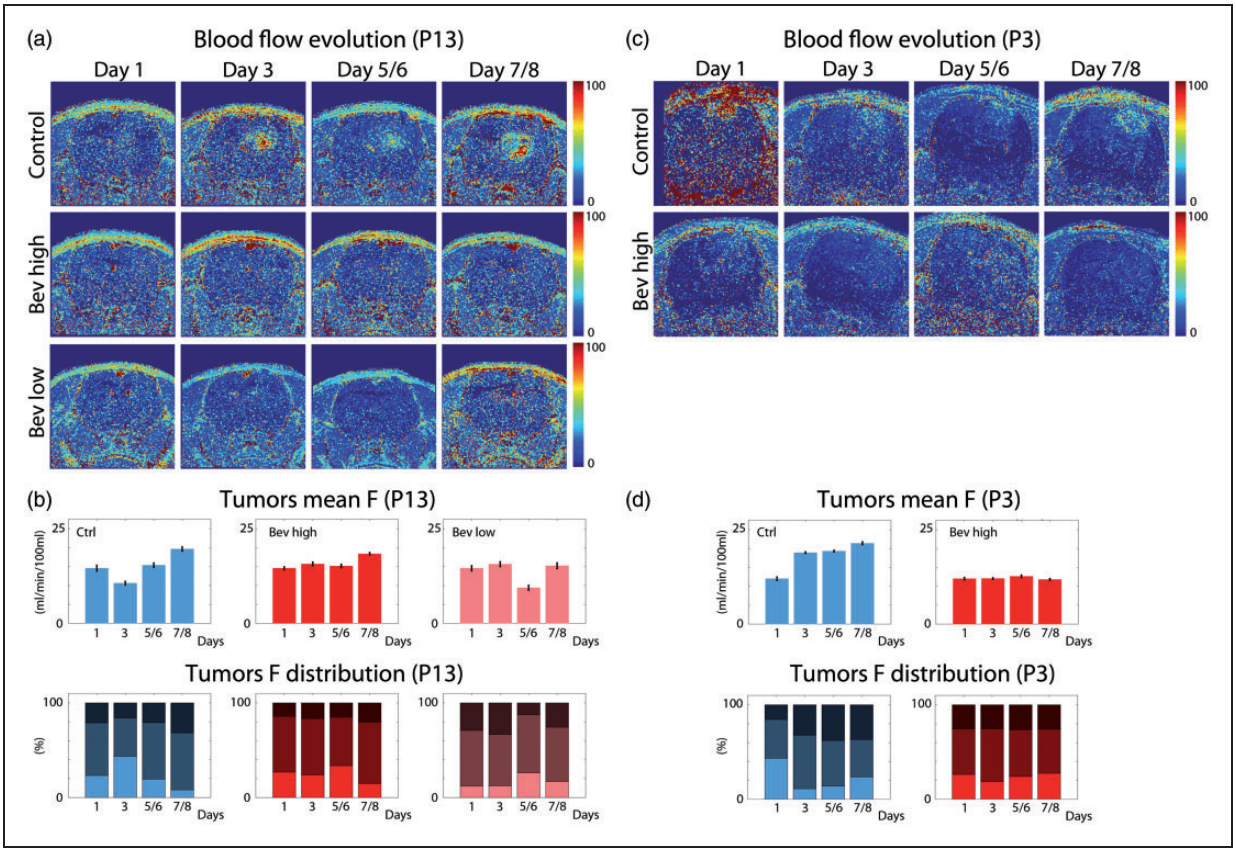

Figure 4. Tumoural blood blow (F) evolution. (a) Illustrative maps of F evolution for animals implanted with the highly angiogenic P13 tumour model, showing one control (top line) and two animals treated with respectively high and low doses of bevacizumab (middle and bottom lines). (b) Quantification of tumour mean F for P13 animals (top line) and histogram analysis of tumour F value distribution (bottom line). In control animals, F is heterogeneous and shows a tendency to increase over time. For animals treated with high or low doses of bevacizumab, F is not improved in comparison to controls and the distribution remains heterogeneous. Similar results can be observed for the less angiogenic more infiltrative P3 model (c and d), suggesting that the morphological normalisation does not result in a functional normalisation with improved and homogenous blood flow. F expressed in absolute values of mL/min/100 mL of tissue. Thresholds for the high, medium and low values (dark, hatched and light blue/red) were defined by the 75% and 25% percentiles of the whole voxels population for the given tumour model. Animals per group: P13 Controls-5, P13 Bev high-5, P13 Bev low-5, P3 Controls-7, P3 Bev high-7. Bev high: 10 mg/kg, Bev low: 5 mg/kg.

the brain than in the tumours. A rigorous comparison would however be hazardous given the somewhat unreliability of parameters estimation in this region with poor SNR.

In summary, the results presented here demonstrate that anti-angiogenic therapy causes a morphological normalisation of blood vessels, evidenced by a statistically significant decrease in tumoural blood volume and vessel permeability, early after the start of the treatment. In this time window however, no functional normalisation was observed in the tumours of the treated animals that would have resulted in an improved blood flow. Instead, tumoural blood flow remains heterogeneous over time, and shows no improvement in comparison to the values observed for the control animals.

Hypoxia

Eight animals implanted with the angiogenic model P13 were used in the PET study, split in controls versus treatment group (bevacizumab high doses). Hypoxia was assessed by ^{18}F-FMISO PET. The signal obtained with this tracer is indeed from hypoxic regions and not healthy tissue since the tracer freely diffuses into all tissues but is only trapped in hypoxic tissue. The optimal timing between injection of the tracer and acquisition was determined from dynamic scans in pilot studies. Longitudinal PET imaging with ^{18}F-FMISO on Day 1, 3, 7 and 12 after treatment start demonstrated a slow increase of the tracer in the control group (Figure 5(a), top line). The uptake of the tracer was strikingly faster in the bevacizumab treated

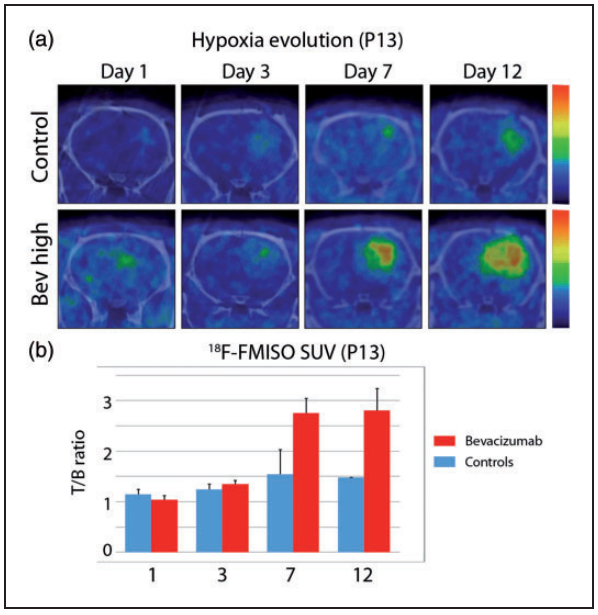

Figure 5. Tumoural hypoxia evolution. (a) Representative images of the longitudinal changes in hypoxia for P13 animals, assessed ^{18}F-FMISO PET, illustrate the high increased uptake of this tracer following treatment with bevacizumab (high dose) compared to the controls. SUV in arbitrary units. (b) Quantification of the ratio of ^{18}F-FMISO standard uptake value (SUV) in tumour versus brain confirms these findings. The following numbers of animals were used (Controls: 4, Bev 10 mg/kg: 4). (Scale bars: SEM).

animals (Figure 5(a), bottom line), accelerating after a few days of treatment. Quantification of the tracer uptake (Figure 5(b)), using the tumour-to-brain ratio of the mean SUV, further confirmed the results. The poor oxygenation of the tumour evidenced here after anti-angiogenic therapy is consistent with the poor tumour perfusion and lack of functional normalisation showed by MRI.

Discussion

As several clinical trials have shown no improvement in OS after treatment of GBM with anti-angiogenic therapy, the focus has now shifted to the identification of the mechanisms of treatment resistance and potential bio- and imaging markers for a subgroup of patients that may respond to this therapy.

Traditionally, the proposed mechanism of action of anti-angiogenic treatment was an inhibition of tumour vessel growth, depriving the tumour of nutrients and oxygen.[12] The vascular normalisation hypothesis emerged as an alternative mechanism of action, through which normalised vessels would lead to an improved blood flow and oxygenation of the tumour.[13,14]

Our group has previously shown that anti-angiogenic treatment with bevacizumab decreases contrast enhancement and blood supply to the tumour in clinically relevant GBM xenografts, increasing hypoxia and invasion.[23] These studies focused on the long-term effects of the therapy, assessed after 3 weeks of treatment with a dose of 10 mg/kg given twice a week. No information was provided then about the short-term effects of the therapy and the possible existence of a window of vascular normalisation early after treatment. In the present work, we addressed this issue by determining dynamic changes in brain tumour perfusion parameters induced by bevacizumab over time, assessed within the first week of treatment. We show that, during this time window, bevacizumab treatment tends to slow down tumour growth, with a more pronounced effect in the purely angiogenic phenotype compared to the mixed angiogenic/infiltrative phenotype. This may reflect an initial treatment response, before adaptation mechanisms occur. We have also previously shown that bevacizumab treatment can lead to an up-regulation of glycolysis, increased lactate accumulation and invasion of tumour cells, possibly highlighting an adaptation mechanism that enables a more infiltrative tumour growth.[23,24]

Using DCE-MRI perfusion analysis, we show that treatment with both high (10 mg/kg) and low (5 mg/kg) doses of bevacizumab leads to a transient normalisation of the vessel morphology, evidenced by stable or marginally decreased blood volume values, and further confirmed this by immunohistochemistry and histology. The treatment also caused a strong decrease in tumour vessel permeability parameters, evidenced by the permeability surface area product PS and the vessel-to-tissue transfer constant K^{trans} that characterises the transport of contrast-agent across the capillary endothelium.[30] At the same time, blood flow did not improve during the time window of the treatment, and remained heterogeneous as evidenced by histogram analysis. This suggests that the morphological normalisation of blood vessels induced by anti-angiogenic therapy was not sufficient to achieve a functional normalisation. The same results were achieved for the two PDX used in the study, which have previously been shown to display purely angiogenic or mixed angiogenic/infiltrative phenotypes.[31] Taken together, these results suggest that poor tumour perfusion and reduced vessel permeability after anti-angiogenic therapy are likely to impede systemic drug delivery, possibly explaining the disappointing results of combined anti-angiogenic/chemotherapy regimens in the clinic so far.[5–7,10]

The method used for perfusion analysis dictates to a large extent the interpretation of putative results obtained. Several reports on the effects of

anti-angiogenic therapy in the brain have used DSC-MRI, a data acquisition method commonly used in the clinic. This approach suffers from the limitation that only relative perfusion parameters can be derived. With this method, blood vessels are also assumed to be non-leaky, such that pre-loading of contrast agent is needed to compensate for the leakiness of blood vessels typically observed in tumours. The contribution of changes in the permeability of blood vessels to the observed changes in blood flow is thus difficult to appreciate with this method. DCE-MRI on the other hand, provides absolute perfusion parameter estimates. Most studies conducted with this method have been based on the (extended) Tofts model for pharmacokinetic analysis, which also makes separation of blood flow from vessel permeability parameter impossible. DCE-MRI, based on the ATH pharmacokinetic model as used in the present study, by introducing one additional parameter in the analysis, makes it however possible to evaluate blood flow and vessels permeability separately. This observation is of importance in the context of treatment with anti-angiogenic agents that are known to modulate the permeability of blood vessels. More information on the methodology used for perfusion analysis in this study is provided in the online Supplementary material, together with examples of raw signal curves and a discussion on the robustness of the model.

Finally, whether DSC-MRI or DCE-MRI is used to derive perfusion parameters maps, averaging blood flow values over the whole tumour may also hide a heterogeneous distribution of blood flow values that would still result in poor perfusion of tumour sub-regions. Histogram analysis of tumoural perfusion parameters values makes it possible to capture this heterogeneity dimension into the analysis, providing additional information to parameters values averaged over the whole tumour. Different studies have started to recognise the role of using histogram and image features analysis to account for the spatial heterogeneity of tumours with benefits related to grading, prognosis and assessment of therapy responses.[32]

In support of our results, a recent clinical study showed no improvement in tumour oxygenation, despite morphological vessel normalisation, assessed in 71 patients with recurrent GBM treated with bevacizumab.[33] Using 18 F-FMISO PET to assess hypoxia, we observed an increased uptake of the tracer both shortly after treatment initiation, and during the first 12 days of treatment, suggesting that the oxygenation of the tumour was decreased rather than increased during the first week of treatment. Poor tumour oxygenation and hypoxia may also contribute to the poor performance of anti-angiogenic therapy combined with standard radio-chemotherapy regimens, by reducing the efficacy of the radiotherapy part of standard GBM treatment.

The observation that bevacizumab treatment decreases contrast enhancement by normalising the vessel morphology, despite the lack of benefit in OS, has been considered of high clinical relevance, as it identified the need for revised radiological response criteria.[8,34,35] Consequently, several studies have tried to identify new radiological biomarkers to predict and measure treatment responses. Schmainda et al.[36] assessed changes in relative cerebral blood volume (rCBV) by DSC-MRI and found that an early decrease in rCBV was predictive of improved survival in patients with recurrent GBM treated with bevacizumab. Other studies have shown that pre-treatment rCBV is a potential predictive biomarker for bevacizumab treatment in patients with recurrent GBM.[30] It has also been proposed that markers derived from diffusion weighted MRI could be used to predict responses to anti-angiogenic therapies.[37,38] ADC has been shown to inversely correlate with cellularity in the brain,[39] providing a potential indicator of infiltrative tumour progression. Indeed, in the study we performed on the long-term effects of bevacizumab,[23] ADC was reduced in the periphery of the tumours suggesting an increased tumour cell infiltration, which was further confirmed by histology. In the present study, changes in ADC values in the tumour periphery early after the start of the treatment were only marginal, suggesting that the evolution to a more infiltrative progression of the tumour is a process that happens at a later stage, after an initial adaptation to treatment.

The bevacizumab dose has also been discussed in the context of vessel normalisation, as it was proposed that lower doses may be more suitable to normalise vessels. A recent meta-analysis revealed that there are no differences in patient outcome whether treated with 10 mg/kg or 5 mg/kg,[40] supporting our results in the present study.

In conclusion, in our orthotopic GBM PDX models, a transient functional window of normalisation of vessels could not be identified following anti-angiogenic therapy. Blood supply to the tumour remains heterogeneous and hypoxia increases while the permeability of tumoural blood vessels is reduced, shedding a causal light on the disappointing results of clinical trials where anti-angiogenic therapies have been combined with systemic delivery of chemotherapeutic agents. This study also shows that MRI combined to PET gives valuable insight into responses to anti-angiogenic therapies, by assessing physiological changes in the tumour in addition to the classically used morphological responses. Such a multimodal imaging approach thus holds a great potential for assessing responses to therapy in both pre-clinical and clinical research.

Funding

The author(s) disclosed receipt of the following financial support for the research, authorship, and/or publication of this article: This work was supported by the Kristian Gerhard Jebsen Foundation, The Research Council of Norway, Stiftelsen Kristian Gerhard Jebsen, Helse Vest, Haukeland University Hospital, the Bergen Medical Research Foundation, the Czech Science Foundation (16-13830S) and the Luxembourg Institute of Health.

Acknowledgements

The MR- and PET-imaging was performed at the Molecular Imaging Center (MIC) and was thus supported by the Department of Biomedicine and the Faculty of Medicine and Dentistry, at the University of Bergen, and its partners. We thank the patients for consenting to donate the tumour tissue and the Department of Neurosurgery at Haukeland University Hospital for the collaboration. We also thank Tina Pavlin for the fruitful discussion on MR protocols optimisation. N Obad was supported by a PhD fellowship from the Norwegian Cancer Society.

Declaration of conflicting interests

The author(s) declared no potential conflicts of interest with respect to the research, authorship, and/or publication of this article.

Access to research materials

Researchers interested in data, samples or models used in the present study are invited to contact the corresponding author.

Authors' contributions

NO, SPN, RB and OK designed the study. NO, HE, POS, CBR, RJ, TT and OK designed the instrumentation, collected and analysed the data. NO drafted the manuscript. NO, HE, MLJ, RJ, TT, SPN, RB and OK revised the manuscript and approved the final version.

Supplementary material

Supplementary material for this paper can be found at the journal website: http://journals.sagepub.com/home/jcb

References

1. Louis DN, Ohgaki H, Wiestler OD, et al. The 2007 WHO classification of tumours of the central nervous system. *Acta Neuropathol* 2007; 114: 97–109.
2. Vredenburgh JJ, Desjardins A, Herndon JE 2nd, et al. Phase II trial of bevacizumab and irinotecan in recurrent malignant glioma. *Clin Cancer Res* 2007; 13: 1253–1259.
3. Kreisl TN, Kim L, Moore K, et al. Phase II trial of single-agent bevacizumab followed by bevacizumab plus irinotecan at tumor progression in recurrent glioblastoma. *J Clin Oncol* 2009; 27: 740–745.
4. Macdonald DR, Cascino TL, Schold SC Jr, et al. Response criteria for phase II studies of supratentorial malignant glioma. *J Clin Oncol* 1990; 8: 1277–1280.
5. Friedman HS, Prados MD, Wen PY, et al. Bevacizumab alone and in combination with irinotecan in recurrent glioblastoma. *J Clin Oncol* 2009; 27: 4733–4740.
6. Chinot OL, Wick W, Mason W, et al. Bevacizumab plus radiotherapy-temozolomide for newly diagnosed glioblastoma. *N Engl J Med* 2014; 370: 709–722.
7. Gilbert MR, Dignam JJ, Armstrong TS, et al. A randomized trial of bevacizumab for newly diagnosed glioblastoma. *N Engl J Med* 2014; 370: 699–708.
8. van den Bent MJ, Vogelbaum MA, Wen PY, et al. End point assessment in gliomas: novel treatments limit usefulness of classical Macdonald's criteria. *J Clin Oncol* 2009; 27: 2905–2908.
9. Reardon DA, Desjardins A, Peters KB, et al. Phase 2 study of carboplatin, irinotecan, and bevacizumab for recurrent glioblastoma after progression on bevacizumab therapy. *Cancer* 2011; 117: 5351–5358.
10. Taal W, Oosterkamp HM, Walenkamp AM, et al. Single-agent bevacizumab or lomustine versus a combination of bevacizumab plus lomustine in patients with recurrent glioblastoma (BELOB trial): a randomised controlled phase 2 trial. *Lancet Oncol* 2014; 15: 943–953.
11. Wick W. Phase III trial exploring the combination of bevacizumab and lomustine in patients with first recurrence of a glioblastoma: the EORTC 26101 trial. *Neuro Oncol* 2015; 17(suppl-5): v1.
12. Folkman J. Tumor angiogenesis: therapeutic implications. *N Engl J Med* 1971; 285: 1182–1186.
13. Jain RK. Normalizing tumor vasculature with anti-angiogenic therapy: a new paradigm for combination therapy. *Nat Med* 2001; 7: 987–989.
14. Carmeliet P and Jain RK. Principles and mechanisms of vessel normalization for cancer and other angiogenic diseases. *Nat Rev Drug Discov* 2011; 10: 417–427.
15. Winkler F, Kozin SV, Tong RT, et al. Kinetics of vascular normalization by VEGFR2 blockade governs brain tumor response to radiation: role of oxygenation, angiopoietin-1, and matrix metalloproteinases. *Cancer Cell* 2004; 6: 553–563.
16. Tong RT, Boucher Y, Kozin SV, et al. Vascular normalization by vascular endothelial growth factor receptor 2 blockade induces a pressure gradient across the vasculature and improves drug penetration in tumors. *Cancer Res* 2004; 64: 3731–3736.
17. McGee MC, Hamner JB, Williams RF, et al. Improved intratumoral oxygenation through vascular normalization increases glioma sensitivity to ionizing radiation. *Int J Radiat Oncol Biol Phys* 2010; 76: 1537–1545.
18. Claes A, Wesseling P, Jeuken J, et al. Antiangiogenic compounds interfere with chemotherapy of brain tumors due to vessel normalization. *Mol Cancer Ther* 2008; 7: 71–78.
19. Arjaans M, Oude Munnink TH, Oosting SF, et al. Bevacizumab-induced normalization of blood vessels in tumors hampers antibody uptake. *Cancer Res* 2013; 73: 3347–3355.
20. Sorensen AG, Emblem KE, Polaskova P, et al. Increased survival of glioblastoma patients who respond to antiangiogenic therapy with elevated blood perfusion. *Cancer Res* 2012; 72: 402–407.

21. Batchelor TT, Sorensen AG, di Tomaso E, et al. AZD2171, a pan-VEGF receptor tyrosine kinase inhibitor, normalizes tumor vasculature and alleviates edema in glioblastoma patients. *Cancer Cell* 2007; 11: 83–95.
22. Batchelor TT, Gerstner ER, Emblem KE, et al. Improved tumor oxygenation and survival in glioblastoma patients who show increased blood perfusion after cediranib and chemoradiation. *Proc Natl Acad Sci U S A* 2013; 110: 19059–19064.
23. Keunen O, Johansson M, Oudin A, et al. Anti-VEGF treatment reduces blood supply and increases tumor cell invasion in glioblastoma. *Proc Natl Acad Sci U S A* 2011; 108: 3749–3754.
24. Fack F, Espedal H, Keunen O, et al. Bevacizumab treatment induces metabolic adaptation toward anaerobic metabolism in glioblastomas. *Acta Neuropathol* 2015; 129: 115–131.
25. Bjerkvig R, Tonnesen A, Laerum OD, et al. Multicellular tumor spheroids from human gliomas maintained in organ culture. *J Neurosurg* 1990; 72: 463–475.
26. Wang J, Miletic H, Sakariassen PO, et al. A reproducible brain tumour model established from human glioblastoma biopsies. *BMC Cancer* 2009; 9: 465.
27. Stieber D, Golebiewska A, Evers L, et al. Glioblastomas are composed of genetically divergent clones with distinct tumourigenic potential and variable stem cell-associated phenotypes. *Acta Neuropathol* 2014; 127: 203–219.
28. Sakariassen PO, Prestegarden L, Wang J, et al. Angiogenesis-independent tumor growth mediated by stem-like cancer cells. *Proc Natl Acad Sci U S A* 2006; 103: 16466–16471.
29. Taxt T, Jirik R, Rygh CB, et al. Single-channel blind estimation of arterial input function and tissue impulse response in DCE-MRI. *IEEE Trans Biomed Eng* 2012; 59: 1012–1021.
30. Kickingereder P, Wiestler B, Graf M, et al. Evaluation of dynamic contrast-enhanced MRI derived microvascular permeability in recurrent glioblastoma treated with bevacizumab. *J Neurooncol* 2015; 121: 373–380.
31. Bougnaud S, Golebiewska A, Oudin A, et al. Molecular crosstalk between tumour and brain parenchyma instructs histopathological features in glioblastoma. *Oncotarget* 2016; 7: 31955–31971.
32. O'Connor JP, Rose CJ, Waterton JC, et al. Imaging intratumor heterogeneity: role in therapy response, resistance, and clinical outcome. *Clin Cancer Res* 2015; 21: 249–257.
33. Bonekamp D, Mouridsen K, Radbruch A, et al. Assessment of tumor oxygenation and its impact on treatment response in bevacizumab-treated recurrent glioblastoma. *J Cereb Blood Flow Metab* 2016; 37(2): 485–494.
34. Wen PY, Macdonald DR, Reardon DA, et al. Updated response assessment criteria for high-grade gliomas: response assessment in neuro-oncology working group. *J Clin Oncol* 2010; 28: 1963–1972.
35. Sorensen AG, Batchelor TT, Wen PY, et al. Response criteria for glioma. *Nat Clin Pract Oncol* 2008; 5: 634–644.
36. Schmainda KM, Zhang Z, Prah M, et al. Dynamic susceptibility contrast MRI measures of relative cerebral blood volume as a prognostic marker for overall survival in recurrent glioblastoma: results from the ACRIN 6677/RTOG 0625 multicenter trial. *Neuro Oncol* 2015; 17: 1148–1156.
37. Pope WB, Kim HJ, Huo J, et al. Recurrent glioblastoma multiforme: ADC histogram analysis predicts response to bevacizumab treatment. *Radiology* 2009; 252: 182–189.
38. Ellingson BM, Cloughesy TF, Lai A, et al. Graded functional diffusion map-defined characteristics of apparent diffusion coefficients predict overall survival in recurrent glioblastoma treated with bevacizumab. *Neuro Oncol* 2011; 13: 1151–1161.
39. Chen L, Liu M, Bao J, et al. The correlation between apparent diffusion coefficient and tumor cellularity in patients: a meta-analysis. *PLoS One* 2013; 8: e79008.
40. Wong ET, Gautam S, Malchow C, et al. Bevacizumab for recurrent glioblastoma multiforme: a meta-analysis. *J Natl Compr Canc Netw* 2011; 9: 403–407.